ELSEVIER

Journal of Alloys and Compounds 271–273 (1998) 327–330

Journal of ALLOYS AND COMPOUNDS

Experimental verification of two deformation paths in the mass division process of actinides

Y.L. Zhao[a,b,*], I. Nishinaka[b], Y. Nagame[b], K. Tsukada[b], M. Tanikawa[c], K. Sueki[a], Y. Oura[a], S. Ichikawa[b], H. Ikezoe[b], T. Ohtsuki[d], H. Kudo[e], H. Nakahara[a]

[a]*Department of Chemistry, Tokyo Metropolitan University, Hachioji, Tokyo 192-03, Japan*
[b]*Japan Atomic Energy Research Institute, Tokai-mura, Ibaraki 319-11, Japan*
[c]*Department of Chemistry, University of Tokyo, Bunkyo-ku, Tokyo 113, Japan*
[d]*Laboratory of Nuclear Science, Tohoku University, Sendai 982, Japan*
[e]*Department of Chemistry, Niigata University, Niigata 950-21, Japan*

Abstract

Double TOF measurements were performed to obtain accurate kinetic energies of fission fragments produced in the proton-induced fission of ^{244}Pu, ^{238}U and ^{232}Th. The presence of two families of the distances between the two complementary fragments at scission, D_{sym} and D_{asym}, is confirmed and their systematic variation from the pre-actinide to the medium actinide region is examined. Variations of the mean total kinetic energies of symmetric and asymmetric mass division products are also studied for a wide range of fissioning nuclides. © 1998 Elsevier Science S.A.

Keywords: TOF measurement; Bimode fission; TKE; Scission configuration; Actinides fission

1. Introduction

In the actinide region, nuclear mass division phenomena are most complicated and it is generally known that they give a double-humped mass yield distribution which cannot be interpreted by the liquid drop behavior of the nucleus. In the beginning of the 1950s, Turkevich and Niday [1] firstly discussed the symmetric and asymmetric fission modes, so called 'two-mode' fission, when studying neutron-induced fission of ^{232}Th. After that, the co-existence of clearly different distributions of symmetric and asymmetric mass division products was observed in the proton-induced fission of ^{226}Ra [2]. Lately, the gross features of symmetric and asymmetric fission phenomena have been extensively investigated and reviewed by many investigators [3–8]. Recently, with the development of the synthesis of heavy elements, the study of the heavy actinide fission became possible, and the presence of bimodal phenomena, namely, two kinds of total kinetic energies (TKE) for the same mass division, was also found [9]. Furthermore, from the studies of low-energy proton-induced fission of ^{232}Th and ^{238}U, the existence of two kinds of total kinetic energies for the same mass division was demonstrated even for the low-energy fission of light actinides, and their correlation with mass division and threshold energies has been clarified [10–12]. Such correlation studies have revealed the presence of at least two independent deformation paths in the fission of light actinide nuclei. One path is characterized by the lower threshold energy and a compact scission configuration resulting in asymmetric mass division. The other one is associated with a higher threshold energy and an elongated scission shape that finally leads to symmetric mass division.

In this work, further studies are carried out to elucidate how the properties of those two deformation paths vary as functions of Z and A of the fissioning nuclide. Some new experimental results of the low energy proton-induced fission of ^{232}Th, ^{238}U and ^{244}Pu will be presented and discussed together with the literature data from the proton-induced fission of ^{209}Bi to the spontaneous fission of ^{260}Md. The discussion will be especially concentrated on the elongation of two adjacent nuclei at scission. In order to avoid the ambiguity resulting from neutron emission from the primary fission products on the measured fragment mass and kinetic energies, double velocity measurements by time-of-flight (TOF) telescopes are used. The

*Corresponding author. E-mail: zhao-yuliang@c.metro-u.ac.jp

PII: S0925-8388(98)00081-4

TKE and the mass yield distribution for each mass split are obtained.

2. Experimental

The ^{232}Th and ^{238}U targets (about 50 μg/cm^2 thickness on 30 μg/cm^2 carbon foils) were prepared by vacuum evaporation, while the ^{244}Pu target (60 μg/cm^2 thickness) was made by electrodeposition onto a 0.1 μm Ni-Cu backing foil. After electroplating, the supporting layer of copper was removed using a $CCl_3COOH+NH_4OH$ etching solution. The proton beams with energies from 10 to 16 MeV were provided by the tandem accelerator at JAERI (Japan Atomic Energy Research Institute). Velocities of complementary fission fragments were measured in coincidence using the double-velocity TOF telescope. The start and stop detectors of TOF1 were both composed of a carbon foil and a microchannel plate (MCP) detector. In TOF2, the start and stop signals were delivered by an MCP and a two-dimensional position sensitive parallel plate avalanche counter (PPAC), respectively. The flight distance of each telescope TOF1 and TOF2 was 50 and 55 cm, respectively. Velocity calibration was carried out by the measurement of elastically scattered and recoil ions from a 240 MeV ^{127}I beam impinging on ^{nat}Ag, ^{nat}In, and ^{209}Bi targets. From the measured velocities of complementary fragments, primary fragment masses and their TKE were determined. The system resolution for mass and energy was determined to be about 2 u and 2.5 MeV, respectively.

3. Results and discussion

As an example of the measured data, the TKE-distributions for fragment mass numbers from A=126 to 132 in the 15 MeV proton-induced fission of ^{232}Th is given in Fig. 1. The measured data are indicated by solid circles. The observed fragment TKE are considered to be the sum of the Coulomb interaction energy between two complementary fragments at scission, the nuclear attractive force still present between the nascent fragments and the prescission kinetic energy arising from the motion from saddle to scission. But the measurable post-scission TKE is approximately equal to the Coulomb repulsion energy, i.e. $TKE=Z_1Z_2e^2/D$, since the energies from the nuclear force and the prescission process nearly cancel [13]. Therefore, D, the distance of charge centers between a pair of complementary fragments at the end of the nuclear deformation process can be estimated from the TKE value measured. In Fig. 2a–e, the results of D as a function of fragment mass number for the proton-induced fission of ^{209}Bi (a), ^{226}Ra (b), ^{232}Th (c), ^{238}U (d) and ^{244}Pu (e) are shown, where the UCD approximation is used for estimating Z_1 and Z_2. The data for the p+^{209}Bi and ^{226}Ra fissions

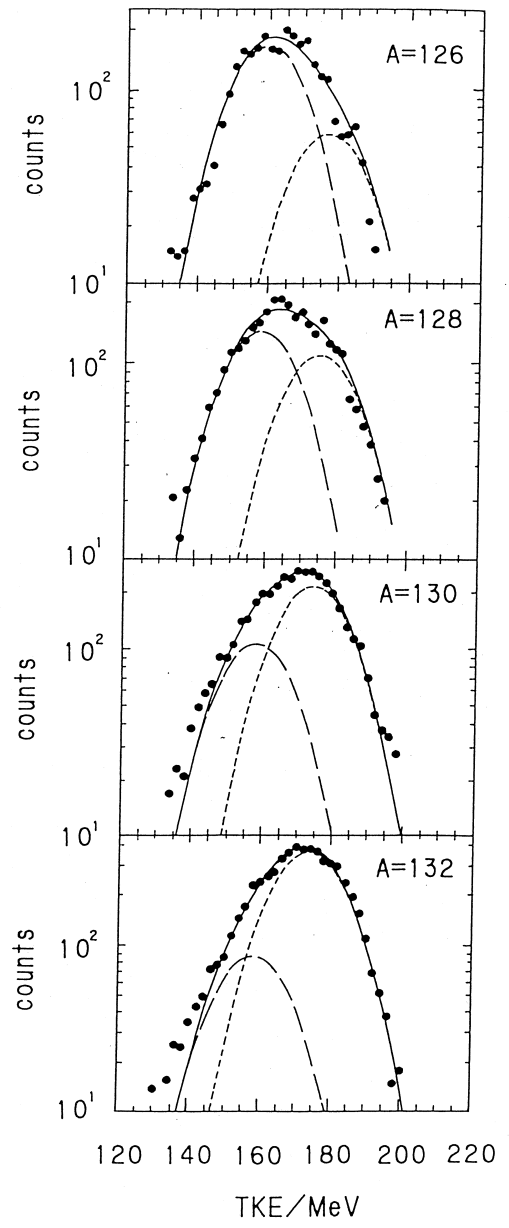

Fig. 1. The TKE-distributions for the fragment masses A=126 to 132 observed in the 15 MeV proton-induced fission of ^{232}Th. The data are shown by solid points. They are decomposed into the low TKE (long-dashed lines) and the high TKE (short-dashed lines) distributions as described in the text.

are taken from M. Tanikawa et al. (personal communication) and [2], respectively. D values evaluated from the mean TKE for each mass division are plotted by solid circles as a function of the heavier fragment mass. From the D-distributions in Fig. 2b–e, it is easy to see that the nuclear elongation at scission can be grouped into three categories. The first group with a larger D (hereafter referred to as D_{sym}) appears in the region of fragment masses less than A=124; the second one has a smaller D (hereafter referred to as D_{asym}) in the fragment mass region beyond A=134, and the third group falls in the inter-

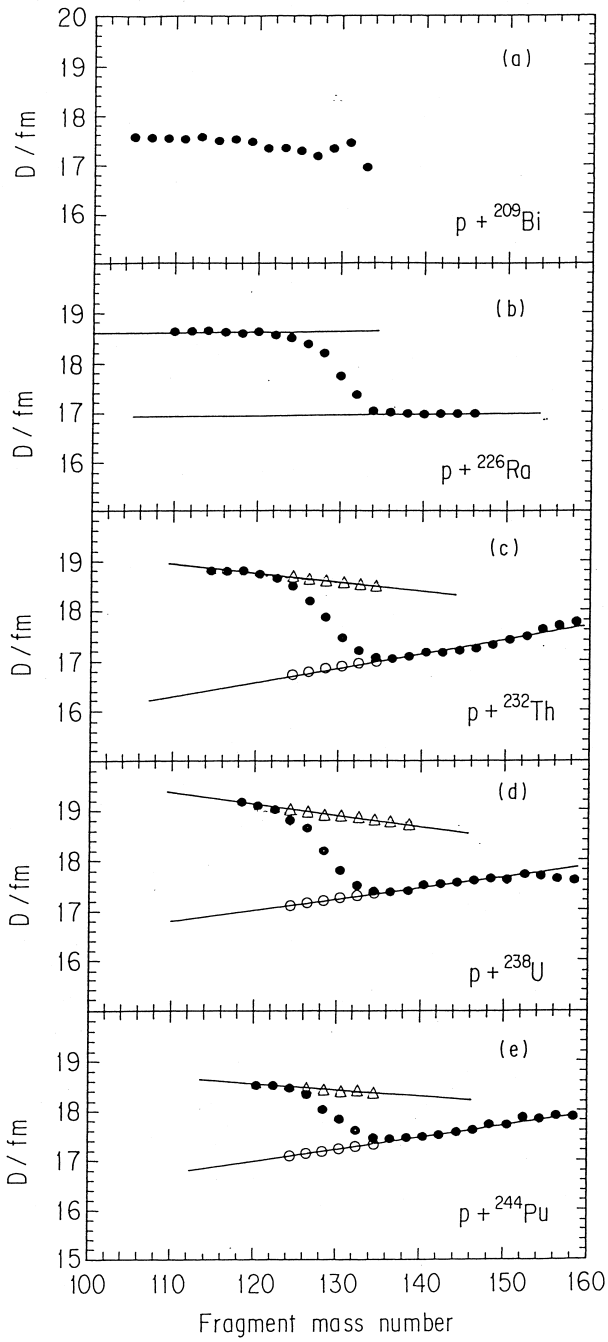

Fig. 2. Distributions of the distance between the charge centers of the complementary fragments in the proton-induced fission of (a) ^{209}Bi, (b) ^{226}Ra, (c) ^{232}Th, (d) ^{238}U and (e) ^{244}Pu, as a function of the heavy fragment mass number. The upper and the lower lines in each figure indicate the *D*-distribution for the symmetric and for the asymmetric mass division modes, respectively. See text for details.

mediate mass region with *D* values (hereafter referred to as D_m) smoothly varying from D_{sym} to D_{asym}. The D_m values are an admixture arising from the other two groups as pointed out in ref. [11], and are decomposed as follows. In Fig. 2, two lines are drawn respectively for the D_{sym} and D_{asym} groups, and both lines are extended to the admixed mass region. The components of D_{sym} and D_{asym} in this admixed region were therefore obtained from these extended lines. They are displayed in Fig. 2c–e by open circles for D_{asym} and by open triangles for D_{sym}. From D_{sym} and $\underline{D_{asym}}$, the corresponding mean values of $\overline{TKE}_{sym}$ and $\overline{TKE}_{asym}$ for each fragment mass number in intermediate region can be estimated, and they can be in turn used for the decomposition of the observed TKE distributions. Results of such a two-Gaussian analysis of the TKE-distributions for the fragment mass A = 126 to 132 are shown in Fig. 1. The long-dashed lines are for the TKE_{sym}- and the short-dashed lines for the TKE_{asym}-distribution, respectively. The solid lines are the sum of the TKE_{sym}- and TKE_{asym}-distributions which are generally in good agreement with the measured overall TKE results shown by the solid dots, which supports the validity of the linear extension of the D_{sym} and D_{asym} lines described above. The general tendency of the D distributions in Fig. 2 can be summarized as follows. (1) As mentioned above, the *D* distributions can be divided into three sections except for p + ^{209}Bi, namely, *D* for symmetric fission products for A ≤ 124, D_{sym}, and *D* for asymmetric fission products for A ≥ 134, D_{asym}, with an intermediate D_m in the mass region of 124 < A < 134. (2) D_{sym} is rather independent of fragment mass A while D_{asym} becomes larger with A. (For ^{226}Ra, data for larger A are missing and a statement on the latter trend is not possible.) (3) The gap between the lines connecting the values of D_{sym} and D_{asym} becomes smaller as the fissioning nuclide becomes heavier.

In Fig. 3, the mean TKE of the total fission, of symmetric and of asymmetric mass division vs. $Z^2/A^{1/3}$ are displayed together with the systematics of Viola et al.

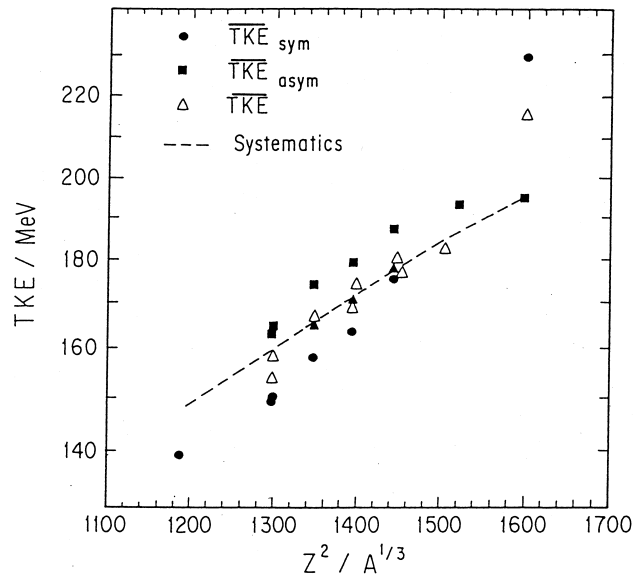

Fig. 3. The dependence on $Z^2/A^{1/3}$ (from the preactinide to the heavy actinide region) of the mean values of TKE released in fission, in the symmetric and asymmetric mass division modes. The solid triangles and their corresponding symmetric and asymmetric values are the present results. The dashed line shows the systematic relation proposed by Viola et al. See text for details.

[14] indicated by the dashed line. The data are the measured $\overline{TKE}$ from the fission of pre-actinides (Bi and Ra), actinides (Th, U, Pu), through the spontaneous fission of heavy actinides, ^{252}Cf [15] and ^{260}Md [9]. The mean TKE of the fission are indicated by the open triangles, and in the case of our own data by the solid triangles. The solid squares and solid circles are the separate $\overline{TKE}$ of the asymmetric and symmetric mass division analyzed in the present work. A study of these data shows that in the pre- and the light-actinide region, the $\overline{TKE}$ released in the symmetric fission is much smaller than the dashed line while the $\overline{TKE}_{asym}$ remain above the dashed line. However, as the fissioning nuclei become heavier, the difference between $\overline{TKE}_{sym}$ and $\overline{TKE}_{asym}$ become smaller, and finally, in ^{260}Md fission, the relative magnitude of $\overline{TKE}_{sym}$ and $\overline{TKE}_{asym}$ is reversed.

4. Summary

Double TOF measurements were newly performed for a very precise determination of primary fragment kinetic energies of the fission fragments produced in the proton-induced fission of ^{244}Pu, ^{238}U and ^{232}Th. The results indicate the presence of the two deformation paths in the studied fission systems. From the observed mean total kinetic energies, the average distance *D* between the two charge centers of the complementary fragments in contact at scission is evaluated for each mass division. A systematic understanding of *D* values from the proton-induced fission of ^{209}Bi up to ^{244}Pu has been attempted, and the presence of completely different families of scission configurations for the symmetric and asymmetric mass division is recognized for a wide range of the fissioning nuclei (more precisely, the compound nuclei) from $^{227}_{89}$Ac to $^{245}_{95}$Am. The mean total kinetic energies of the symmetric and asymmetric mass division products, $\overline{TKE}_{sym}$ and $\overline{TKE}_{asym}$ are plotted as a function of $Z^2/A^{1/3}$ of the fissioning nuclides, and they are compared with the empirical relation proposed by Viola et al. The $\overline{TKE}_{asym}$ is larger than $\overline{TKE}_{sym}$ in the region of ^{227}Ac through ^{245}Am, but the difference between the two becomes smaller as the fissioning nucleus becomes heavier, thus allowing for the possibility of $\overline{TKE}_{sym}$ to become larger than $\overline{TKE}_{asym}$ in the heavy actinide region as actually reported for the spontaneous fission of ^{260}Md and ^{258}Fm.

Acknowledgements

We are very grateful to the operating staff of the JAERI Tandem Accelerator for providing the beam.

References

[1] A. Turkevich, J.B. Niday, Phys. Rev. 84 (1951) 52.
[2] E. Konecny, H.W. Schmitt, Phys. Rev. 172 (1968) 1213.
[3] For example, E.K. Hyde, Nuclear Properties of the Heavy Elements, vol. 3, Prentice-Hall, NJ, 1964.
[4] H.R. von Gunten, Actinides Rev. 1 (1969) 275.
[5] R. Vandenbosch, J. Huizenga, Nuclear Fission, Academic Press, New York, 1973.
[6] H.C. Britt, Physics and Chemistry of Fission 1979, vol. 1, IAEA, Vienna, 1980, pp. 3–29.
[7] H. Nakahara, T. Ohtsuki, J. Radioanal. Nucl. Chem, Articles 142 (1990) 231.
[8] D.C. Hoffman, M.R. Lane, Radiochem. Acta 70–71 (1995) 135.
[9] E.K. Hulet, J.F. Wild, R.J. Dougan, R.W. Lougheed, J.H. Landrum, A.D. Dougan, M. Schädel, R.L. Hahn, P.A. Baisden, C.M. Henderson, R.J. Dupzyk, K. Sümmerer, G.R. Bethune, Phys. Rev. Lett. 56 (1986) 313.
[10] T. Ohtsuki, Y. Nagame, H. Ikezoe, K. Tsukada, K. Sueki, H. Nakahara, Phys. Rev. Lett. 66 (1991) 17.
[11] Y. Nagame, I. Nishinaka, K. Tsukada, Y. Oura, S. Ichikawa, H. Ikezoe, Y.L. Zhao, K. Sueki, H. Nakahara, M. Tanikawa, T. Ohtsuki, H. Kudo, Y. Hamajima, K. Takamiya, Y.H. Chung, Phys. Lett. B387 (1996) 26.
[12] Y. Nagame, I. Nishinaka, K. Tsukada, S. Ichikawa, H. Ikezoe, Y.L. Zhao, Y. Oura, K. Sueki, H. Nakahara, M. Tanikawa, T. Ohtsuki, K. Takamiya, K. Nakanishi, H. Kudo, Y. Hamajima, Y.H. Chung, Radiochim. Acta (1997) (in press).
[13] B.D. Wilkins, E.P. Steinberg, R.R. Chasman, Phys. Rev. C 14 (1976) 1832.
[14] V.E. Viola, K. Kwiatkowski, M. Walker, Phys. Rev. C 31 (1985) 1550.
[15] H.W. Schmitt, W.E. Kiker, C.W. Williams, Phys. Rev. 137 (1965) B873.